

Reprint from "Siemens-Review"

Vol. XXXIV · February 1967 · No. 2 · Pages 60 to 68

Authors: Karl Heintz and Erich Mayerhofer

More than a year has passed since conventional long-range communications systems operating over marine cables or shortwave and longwave radio paths were joined by the first satellite communications systems. In the near future, the application of the multi-channel approach to satellites will lead to their more widespread use in radiocommunication, especially for the following four primary applications:

Intercontinental and continent-wide links for the transmission of telephone conversations, teleprinter messages, data, and radio and television programs.

Communications within large countries still without a nationwide radio relay or cable network of their own, e. g. developing countries.

Expansion of existing radio relay networks in large countries, e. g. the USA.

Military radiocommunication, especially with mobile earth stations, in the frequency range from 7.9 to 8.5 ghz.

Used in radio relay networks the satellite acts as a repeater. Signals from an earth station are picked up by the satellite, converted to another frequency, amplified, and retransmitted to another earth station. The frequency bands 5.725 to 6.425 ghz (with preferred use of the band 5.925 to 6.425 ghz) and 7.9 to 8.4 ghz have been allocated for earth-to-satellite transmission and the bands 3.4 to 4.2 ghz and 7.25 to 7.45 ghz for satellite-to-earth transmission.

Since the great distance between earth stations and the satellite results in a very high path loss, the earth stations must be equipped with high-power transmitters. The power required per carrier may be estimated as follows:

Experience has shown a radiated power of 58 dbw¹ per voice channel to be sufficient. Using this figure as a basis of calculation, single-carrier operation with 120 channels and an antenna with a gain of 60 db calls for a final power stage with a maximal power (referred to 1 watt) of 58 dbw + 20.8 db (120 channels) + 5 db (increment allowing for bad weather and feed losses) - 60 db (antenna gain), which corresponds to 240 watts.

On choosing the final power stage of the transmitter for earth stations

Satellite radiocommunication has hitherto been restricted to intercommunication between two earth stations, with each station transmitting and receiving a single frequency-modulated carrier. Klystrons or traveling-wave tubes were used as transmitting amplifiers. For small-band

single-carrier operation, klystrons are equivalent to traveling-wave tubes in transmission performance, whereas in gain and operating costs they are superior. Broadband frequency-modulated signals such as frequency modulated television signals with a bandwidth of 40 Mhz, however, can only be boosted with a traveling-wave tube without serious distortion.

Transmission systems now under development will allow simultaneous intercommunication between several earth stations by way of a satellite. Each earth station must for this purpose be able to radiate several frequency-modulated carriers simultaneously, the various carrier frequencies being chosen in the 6-ghz directional radio band according to a frequency allocation established by COMSAT (**C**ommunications **S**atellite Corporation). Carriers radiated from an earth station may be amplified either *in common* by way of a *single transmitter tube* or *individually* by way of a *separate tube* for each. Here again a broadband traveling-wave tube will be eminently suitable because only two tubes in all would have to be provided for standby operation and reserve. If narrow-band tubes were used it would be necessary in the case of operation with several carriers to assign to each carrier a previously tuned tube for standby operation and another as a reserve.

Used in earth stations, traveling-wave tubes further offer the advantage that more channels may be added to the communications system without greatly increasing the cost of the final power stage, and that the transmitting frequency can be changed very rapidly.

The transmitter power required for multi-carrier operation may be calculated with the aid of the rule-of-thumb formula already given. This means that, say, four carriers with 120 channels each will require a maximal power (referred to 1 watt) of 58 dbw (power per channel) + 20.8 db (120 channels) + 6 db (4 carriers) + 5 db (increment allowing for bad weather and feeding losses) - 60 db (antenna gain), corresponding to about 1 kw. To ensure low-distortion in four-carrier operation, the saturation power of the final power stage must be 4 kw, i.e. about 6 db above this maximal power.

The Siemens traveling-wave tube YH 1041 is now available as a broadband transmitter tube with a saturation power of 5 kw. Operated in the frequency range of 5.925 to 6.425 ghz with one or more carriers and stabilized operating voltages, the tube delivers average c-w power

1 The term "*n* dbw" means that the difference between a given power *P* and the reference power value 1 watt is *n* db ($10 \log P/1 = n$), e. g. 20 dbw corresponds to a power of 100 watts.

of up to 3 kw. Its efficiency is in this case about 25% and the gain at the edges of the band about 30 db. The delay-line voltage remains constant within the 6-ghz directional radio band irrespective of the carrier frequencies. Table 1 gives the principal operating data of the new tubes.

Design of traveling-wave tube YH 1041

Fig. 1 shows a cutaway section of the traveling-wave tube YH 1041. This tube has the same outer dimensions and mechanical design as its predecessor, the 2-kw type YH 1040 used in the transmitter stage of Raisting earth station [1, 2, 3], but owing to its higher output power and consequently higher radiated power its delay-line structure and electron gun are designed differently.

An 8-mm dispenser cathode is provided for generating the electron beam. The beam voltage E_{d1} is 18 kv and the beam current I_{cat} about 1.4 amp. The beam is focused with electrostatic and magnetic fields to a radius of about 3 mm [2]. In designing the *electron gun*, special attention was devoted to ensuring that the thermal emission of the negative beam-shaping electrode to the cathode and to the anode remains sufficiently small. The beam-shaping electrode is for this purpose coated with a metal with an extra-high work function: in addition, the temperature of this electrode is kept as low as possible through the use of a mount designed for good heat conduction.

Beam-focusing is effected by a periodic magnetic field, a feature which has already proved its value with the 2-kw traveling-wave tube YH 1040. The magnet system (Fig. 2a, b) consists of two rows of soft-iron pole pieces magnetized by four Alnico V plates. It is divided in two in its symmetrical plane and mounted on two hinges. The beam is formed by a magnetic field of adjustable positive and negative amplitude. As compared with a monotonously increasing field, this field has the advantage that both convergent and divergent electron beams may be adapted to the main magnetic field. With a periodic field the outer stray magnetic field is far weaker and the weight and bulk of the magnet less than that of a corresponding constant-field permanent magnet. The constructional design of the periodic magnet allows axial inductions of more than 1,000 g if the induction in the iron is about

Frequency range	5.925 to 6.425	ghz
Output power P_o	3	kw
Gain G	30	db
Heater voltage E_f	6.7	v
Heater current I_f	2.6	amps
Anode voltage E_{e2}	3.5	kv
Beam-shaping electrode voltage E_{e1}	300	v neg
Delay-line voltage E_{d1}	18	kv
Delay-line current I_{d1}	to 150	ma
Collector voltage E_b	11 to 13	kv
Collector current I_b	1.4	amps

Table 1 Principal operating data of the traveling-wave tube YH 1041

20,000 g. The peak induction values for the tube YH 1041 are around 900 g. The temperature sensitivity of the induction is low (0.3 g/deg). A field straightener (Fig. 2a) is fitted over the delay-line structure in order to suppress the disturbing transversal fields which cannot be avoided owing to the inevitable production tolerances. Such fields would impair the quality of beam focusing. The field straightener consists of soft-iron rings (blue and red) of different length interconnected by non-magnetic spacer rings (green). The transversal field components are reduced by rings (red) interposed between the pole pieces (gray). Fig. 2c shows the influence of the rings on the transversal field at the point $B_{z\max}$ as a function of the angle φ .

The water-cooled *collector* (maximum permissible inlet temperature of water 60°C, flow rate 30 ltr/min) is so designed that r-f radiation is largely suppressed. The total power of the r-f radiation over an area of about 60 cm² amounts to only a few milliwatts. The collector voltage is about 7 kv lower than the beam voltage applied to the delay line. Thus the dissipation dispersed as heat is reduced and, as with the tube YH 1040 [2], the total efficiency of the tube increased without any appreciable impairment of the r-f characteristics and the loss current on the delay line.

Developed from a backward-wave oscillator circuit, the *delay line* of the tube YH 1041 consists, as with the tube

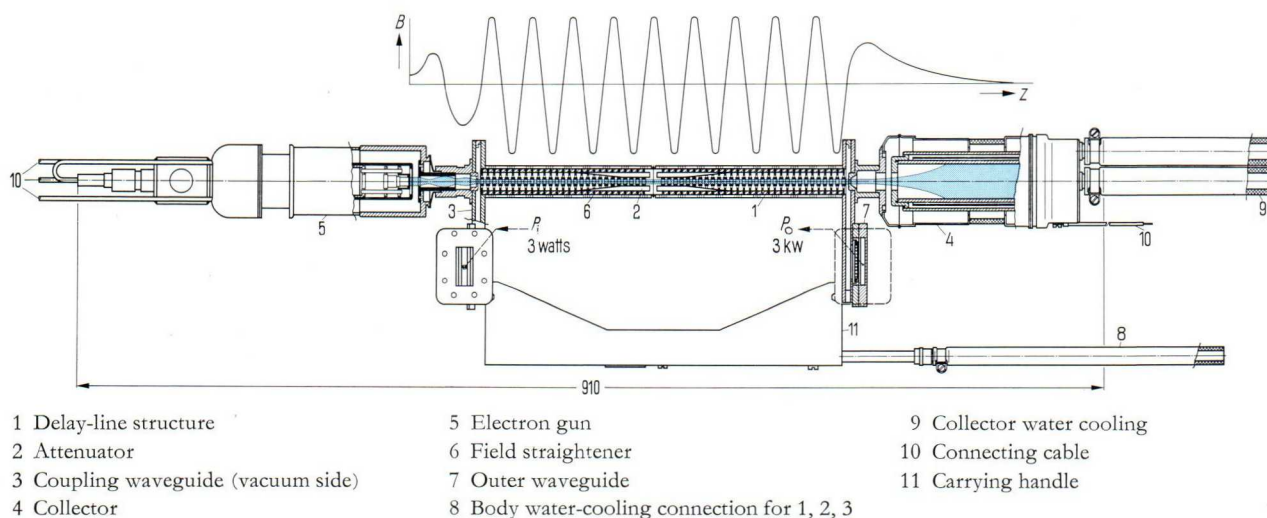


Fig. 1 Traveling-wave tube YH 1041. Top: Magnetic field for periodic focusing. Bottom: Longitudinal section through tube

YH 1040, of coupled cavity resonators. It is dimensioned so that the tube will withstand a dissipation of 3 kw and remains free of r-f oscillations while the operating voltages are building up [3]. A flow rate of 4 ltr/min is required for water-cooling the delay-line structure; the maximum inlet temperature of the water is again 60 °C.

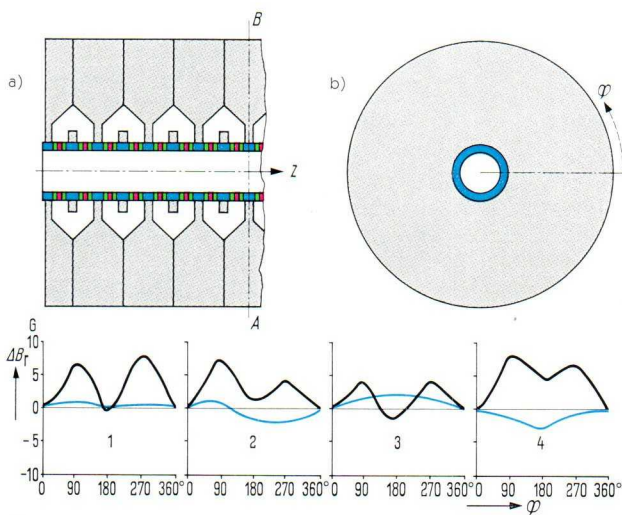
The r-f power is fed in and coupled out by way of *rectangular waveguides* WR 137 and vacuum-tight *ceramic windows* provided in the broad side of the waveguides. The windows are so arranged that only a single type of mode is excited throughout the operating frequency range. Owing to their favorable geometry, the windows rise in temperature by only about 35 deg for an output power of 3 kw and so do not require air-cooling.

Wedge-shaped *attenuators* fabricated by sintering a mixture of metal powder with ceramic powder are used for localized attenuation. Since life tests have shown these attenuators to retain their crystal structure even when exposed to temperature cycling, constant r-f matching is ensured during the life of the tube. Being of great mechanical strength, the attenuators may be brazed directly to the wall of the delay-line structure, so securing extremely good heat conduction.

Operating data of the traveling-wave tube YH 1041

Placing in service

In designing the tube YH 1041 and its magnet system, care was exercised to ensure that it inserts easily and



a) Magnet system, longitudinal section
 b) Magnet system, cross section *AB*
 Blue: Soft-iron rings
 Green: Non-magnetic spacer rings
 Red: Soft-iron rings
 Gray: Pole piece
 φ Position coordinate
 c) Deviation of induction from the expected fixed value of induction B_r due to the rotational symmetry of the arrangement, as a function of the angle φ in four gaps (1, 2, 3, 4)
 Black: Without field straightener
 Blue: With field straightener

Fig. 2 Magnetic transversal fields of traveling-wave tube YH 1041 with and without field straightener

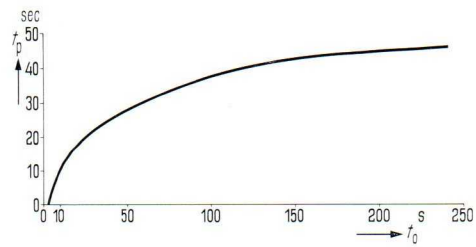


Fig. 3 Preheating time t_p of traveling-wave tube 1041 as a function of the duration t_o of the outage of heating power

quickly in the magnet system. Since it aligns itself automatically on insertion, its position does not have to be corrected once the magnet system is closed.

When the tube is placed in service for the first time and the entrance of the beam into the periodic magnetic field is optimally adjusted with correction magnets, starting may be initiated by the customer according to the given instructions. After an interruption of operation, the preheated tube (preheating time 5 min) may be turned on as quickly as the power supply allows. This is likewise possible in the presence of r-f input power.

Even in the absence of driving power, the tube may only be operated with its input and output waveguides terminated with low reflection. Thus a circulator must be attached to both ends of the tube to protect it from strong reflections as may occur, say, when the waveguide switch is actuated. The circulator must be adapted for use in the frequency range of 5.6 to 6.5 ghz; the voltage reflection coefficient must not exceed 20% in the range from 5.925 to 6.425 ghz, i.e. no more than 120 watts must be reflected when the tube is driven with 3 kw. The circulator at the output must be dimensioned for a power of 3 kw; the reverse attenuation should be greater than 20 db. The circulator at the input serves primarily for protecting the driver stage in the presence of possible oscillation at the input (e.g. towards the end of the tube's service life). It must be able to withstand a c-w power of about 200 watts in the reverse direction for at least a few seconds. The output circulator also prevents a reflected wave from returning to the tube in the event of a flashover in the feeder waveguide of the antenna.

Standby circuit

A standby tube may be connected in parallel with the regular tube so that it may take over if the latter fails. Transmission is interrupted during the changeover from one tube to the other. Depending on whether the standby tube is only preheated or already available with full voltages applied, the changeover time will be either a few seconds (buildup time of high voltages), or about 200 msec (actuation of waveguide switch).

After a brief failure of all the voltages (including the heating voltage) the tube YH 1041 may be turned on again after the preheating times read off in Fig. 3, whereas with interruptions of up to 3 sec in duration the full voltages may be applied immediately.

Replacement of tube

The tube may be replaced in a matter of about an hour. If the new tube has been on the shelf for a lengthy period, a further hour will elapse before it attains its full operating output power, during which time the beam

may be positioned and residual gases, if any, absorbed. No readjustment of the r-f matching is necessary when a new tube is inserted.

R-f characteristics of traveling-wave tube YH 1041

Bandwidth

Assuming a stable circuit voltage and input power, the 3-db bandwidth of the tube YH 1041 will extend from 450 to 500 Mhz. If the ripple content of the voltage applied to the gun and delay line is about 0.1 to 0.2%, the amplitudes of the output signal vary by less than 0.1 db.

The black curve in Fig. 4 shows the frequency response of the gain G for constant values of the delay-line voltage and an input power in the frequency range of 5.925 to 6.425 ghz. If the input powers are suitably chosen, the operating output power of 3 kw will be attained throughout the 6-ghz band allocated to radio relay systems. The gain slope of the tube is less than 0.03 db/Mhz.

If several carriers within the 6-ghz band have to be amplified simultaneously, the delay-line voltage should be adjusted so that optimal transmission conditions are obtained for all carriers. The input powers of the individual carriers should be set according to the frequency response of the gain of the tube. When the tube is turned on, there is no need for any frequency-determining element within the frequency band to be readjusted.

The quality of transmission is further influenced by non-linear distortion and noise. CCIR recommendations exist covering the permissible noise powers.

Distortion

Two types of distortion occur when traveling-wave tubes are driven with one or more signals:

Amplitude distortion (expressed in percentile compression c) produced by a nonlinear relationship between the input power and the output power.

Phase distortion (amplitude-phase conversion expressed as a-m/p-m conversion coefficient c_p in degrees per db) produced by the dependence of the phase of the output signal on the input loading of the tube. With increasing output power the electron beam is progressively retarded, thereby resulting in delay times that are dependent on the power.

As a first approximation the third-order intermodulation distortion (in db) resulting from the two forms of distortion when the tube is loaded with two signals is [4, 5]:

$$D_3 = 40 - 10 \log \left[\left(\frac{c}{8} \right)^2 + (1.9 c_p)^2 \right] \quad (1)$$

where

$$c = \left(1 - \frac{\Delta V_o / V_o}{\Delta V_i / V_i} \right) 100\%$$

where V_i and V_o denote the input and output r-f voltages. The values c and c_p in equation (1) are referred to peak values of the output power.

Compression with multi-carrier operation

When a traveling-wave tube is operated with n carriers of equal power, the peak values \hat{P} of the powers may be calculated with the aid of the equations

$$\hat{P} = 2n \bar{P}_{tot} \quad \text{or} \quad (2a)$$

$$\hat{P} = 2n^2 \bar{P}_s \quad (2b)$$

where P_{tot} is the total average power of all the carriers measured with, say, a calorimeter, and \bar{P}_s is the average power of a single carrier. This means that whereas the peak value for a single carrier can always only assume twice the value of the average power of that carrier, with simultaneous operation with two carriers it already attains theoretically four times the value of the measured total average power. The power peaks appear whenever the instantaneous values of the voltages of the individual carriers are *in phase* and so attain peak values (Fig. 5). The larger the number of carriers n , the more seldom this state will occur. In consequence, the sum power attains the theoretically possible peak value less frequently with $n \geq 3$ than with $n = 2$.

The gain of the tube YH 1041 during operation with one or more carriers is illustrated in Fig. 6 by showing the average value \bar{P}_o of the output power plotted over the average value \bar{P}_i of the input power. Having regard for the frequency response of the gain, the input powers have been so chosen that all the carriers have the same output powers. The phenomenon that the decrease in gain with a consequent increase in compression begins earlier with increasing numbers of carriers is due to the fact that higher peak power values result during operation with several carriers. In the case of the tube YH 1041 the power peaks beyond about 4 kw are compressed and, when a peak value of 8 to 10 kw ($c = 100\%$) is reached, cut off.

Since inphase carrier amplitudes occur more frequently with two-carrier operation than with operation with

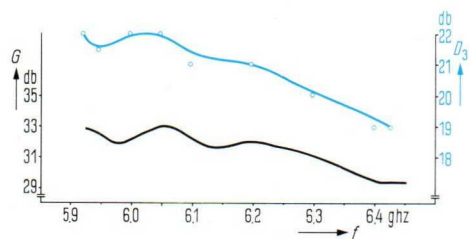


Fig. 4 Frequency response of the gain G (black) of the traveling-wave tube YH 1041 with constant delay-line voltage and input power ($P_i = 0.8$ watt) and of the third-order intermodulation distortion $D_{3.2}$ (blue) for an total average output power of 1.3 kW

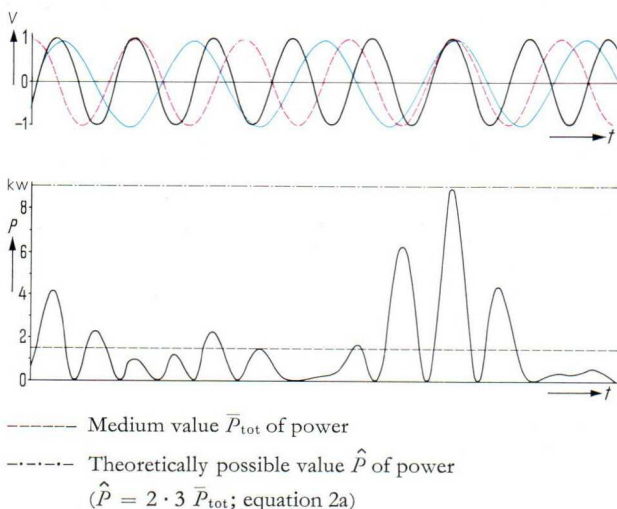
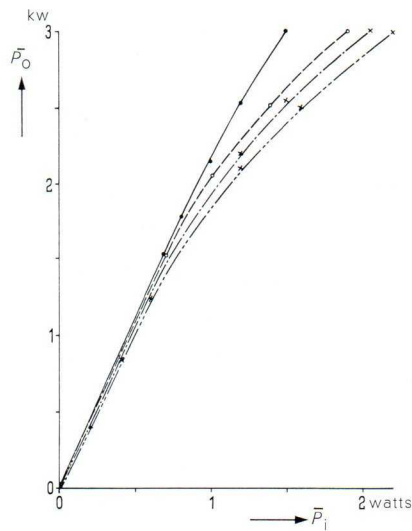


Fig. 5 Voltage V and total power P as a function of time for linear operation of a tube with three carriers (black, red, blue)

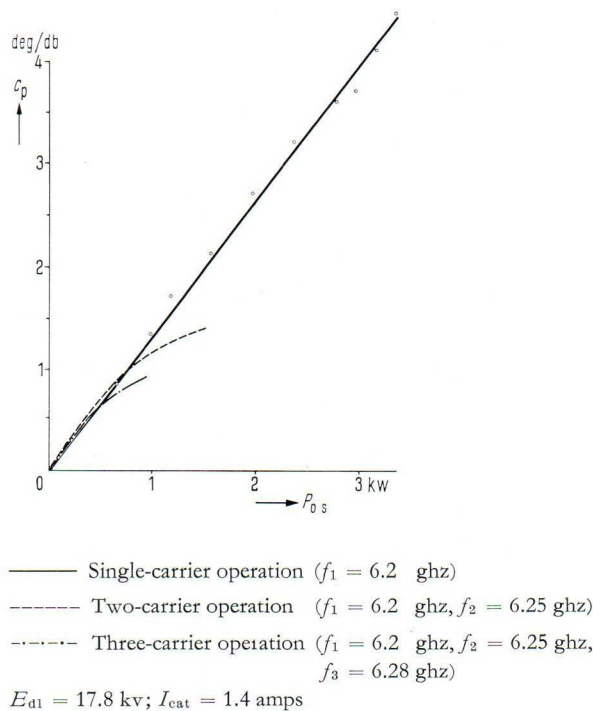
three or more carriers, the decrease in gain on changing from one to two carriers is greater than on changing from two to three carriers.

Table 2 gives the compression values for operation with one, two, three and four carriers and three different values of the sums of the average carrier powers.



— Single-carrier operation ($f_1 = 6.3$ ghz)
 - - - Two-carrier operation ($f_1 = 6.3$ ghz, $f_2 = 6.305$ ghz)
 - · - · Three-carrier operation ($f_1 = 6.3$ ghz, $f_2 = 6.305$ ghz, $f_3 = 6.31$ ghz)
 · · · · Four-carrier operation ($f_1 = 6.3$ ghz, $f_2 = 6.305$ ghz, $f_3 = 6.31$ ghz, $f_4 = 6.39$ ghz)
 $P_{o1} = P_{o2} = P_{o3} = P_{o4}$; $E_{d1} = 17.8$ kv; $I_{cat} = 1.4$ amps

Fig. 6 Average value \bar{P}_o of output power as a function of the average value \bar{P}_i of the input power for multi-carrier operation of the tube YH 1041



— Single-carrier operation ($f_1 = 6.2$ ghz)
 - - - Two-carrier operation ($f_1 = 6.2$ ghz, $f_2 = 6.25$ ghz)
 - · - · Three-carrier operation ($f_1 = 6.2$ ghz, $f_2 = 6.25$ ghz, $f_3 = 6.28$ ghz)
 $E_{d1} = 17.8$ kv; $I_{cat} = 1.4$ amps

Fig. 7 Influencing of the a-m/p-m conversion coefficient c_p of a carrier by one and two additional carriers

Amplitude-phase conversion in multi-carrier operation

The phase-modulation (p-m) of an amplitude-modulated (a-m) signal is characterized by the change in phase (in deg) for the change in power (in db) [5].

Fig. 7 shows how the a-m/p-m conversion coefficient c_p of a single carrier (solid line) is influenced by *one additional* carrier (dashed line) and by *two additional* carriers (dashed-dotted line). For an output power of 3 kw in single-carrier operation, $c_p \approx 4$ deg/db; if the angular change expressed in radians and the change in power of 1 db is given in a linear ratio, then c_p is ≈ 0.6 . If a second carrier is present and the average powers of the individual carriers are more than 0.7 kw, the values of c_p will differ slightly from those for single-carrier operation. With a power of 1.5 kw per carrier, for example, c_p will be about 0.5 deg/db smaller. The reason for this is that if two carriers are present simultaneously the tube will be driven more in the saturation region, so that any change in the amplitude of the input signal will no longer seriously affect the output signal.

Third-order intermodulation distortion

Operation with two carriers

If a nonlinear four-terminal network is operated with two signals of different frequency, intermodulation products with the frequencies

$$f_{pq} = pf_1 \pm qf_2 \quad (3)$$

will appear at the output in addition to the two carriers¹. The order of the intermodulation product is determined by the addition of the integrals p and q ($p > 0, q > 0$). In the case of $p = 2$ and $q = 1$ or $p = 1$ and $q = 2$, reference is made to a third-order intermodulation product with the third-order intermodulation distortion $D_{3,2}$.

With a traveling-wave tube the *difference* frequencies $2f_1 - f_2$ and $2f_2 - f_1$ usually lie within the passband of the tube. The intermodulation products with the *sum* frequencies $2f_1 + f_2$ and $2f_2 + f_1$ fall in the region of the third harmonic and may be neglected. The same applies to the intermodulation products of fifth or higher order, for their amplitudes are usually more than 10 db smaller than those of third-order products.

The third-order intermodulation distortion $D_{3,2}$ due to intermodulation products with difference frequencies deriving from two carriers equals the ratio of the average power of a single intermodulation product having one of these difference frequencies to the average power of a single signal with one of the fundamentals.

1 The nonlinear voltage characteristic may be described by an equation having the form $V_o = a_0 + a_1 V_i + a_2 V_i^2 + a_3 V_i^3 + \dots + a_n V_i^n$ (the subscripts o and i denote output and input). In practice this equation may be curtailed after the third-order term. The influence of phase distortions is neglected for the sake of simplicity, for it may be shown that these will not be responsible for any new intermodulation frequencies and that only the amplitudes of the intermodulation products undergo a change. For two-carrier operation

$$V_i = V_{i1} + V_{i2} = A_1 \cos 2\pi f_1 t + A_2 \cos 2\pi f_2 t,$$

so that for amplitude equality ($A_1 = A_2 = A$)

$$V_o = a_0 + \dots + \frac{1}{4} a_3 A^3 \cos 2\pi (3f_1)t + \frac{1}{4} a_3 A^3 \cos 2\pi (3f_2)t + \frac{3}{4} a_3 A^3 \cos 2\pi (2f_1 + f_2)t + \frac{3}{4} a_3 A^3 \cos 2\pi (2f_1 - f_2)t + \frac{3}{4} a_3 A^3 \cos 2\pi (2f_2 + f_1)t + \frac{3}{4} a_3 A^3 \cos 2\pi (2f_2 - f_1)t$$

2 For three-carrier operation, $V_i = V_{i1} + V_{i2} + V_{i3} = A_1 \cos 2\pi f_1 t + A_2 \cos 2\pi f_2 t + A_3 \cos 2\pi f_3 t$, so that for amplitude equality ($A_1 = A_2 = A_3 = A$) $V_0 = a_0 + \dots + \frac{1}{4} a_3 A^3 [\cos 2\pi (3f_1)t - 3 \cos 2\pi f_1 t] + \frac{1}{4} a_3 A^3 [\cos 2\pi (3f_2)t - 3 \cos 2\pi f_2 t] + \frac{1}{4} a_3 A^3 [\cos 2\pi (3f_3)t - 3 \cos 2\pi f_3 t] + \frac{3}{4} a_3 A^3 [2 \cos 2\pi f_2 t + \cos 2\pi (2f_1 - f_2)t + \cos 2\pi (2f_1 + f_2)t] + \frac{3}{4} a_3 A^3 [2 \cos 2\pi f_1 t + \cos 2\pi (2f_2 - f_1)t + \cos 2\pi (2f_2 + f_1)t] + \frac{3}{4} a_3 A^3 [2 \cos 2\pi f_1 t + \cos 2\pi (2f_3 - f_1)t + \cos 2\pi (2f_3 + f_1)t] + \frac{3}{4} a_3 A^3 [2 \cos 2\pi f_2 t + \cos 2\pi (2f_3 - f_2)t + \cos 2\pi (2f_3 + f_2)t] + \frac{3}{4} a_3 A^3 [2 \cos 2\pi f_3 t + \cos 2\pi (2f_2 - f_3)t + \cos 2\pi (2f_2 + f_3)t] + \frac{3}{2} a_3 A^3 [\cos 2\pi (f_2 + f_3 - f_1)t + \cos 2\pi (f_1 + f_3 - f_2)t + \cos 2\pi \times (f_1 + f_2 - f_3)t + \cos 2\pi (f_1 + f_2 + f_3)t]$

\bar{P}_0 kw	c %				
	$n =$	1	2	3	4
1.5	0	10	13	19	
2	10	26	29	34	
3	34	40	43	46	

Table 2 Compression values for multi-carrier operation of traveling-wave tube YH 1041

Operation with three or more carriers

When a nonlinear amplifier is operated with three carriers², three intermodulation products with the difference frequencies $f_2 + f_3 - f_1$, $f_1 + f_3 - f_2$ and $f_1 + f_2 - f_3$ appear in addition to the six intermodulation products with the difference frequencies $2f_1 - f_2$, $2f_2 - f_1$, $2f_3 - f_1$, $2f_1 - f_3$, $2f_3 - f_2$ and $2f_2 - f_3$, which by their definition determine the intermodulation distortion $D_{3,2}$ (Fig. 8). The calculation shows that the voltage amplitudes of these six and the three previously recorded intermodulation products are in a ratio of $3/2 : 3/4 = 2 : 1$, which means that the powers are in a ratio of 4:1, corresponding to the power ratio of 6 db.

The third-order intermodulation distortion $D_{3,3}$ due to the appearance of intermodulation products with difference frequencies deriving from three carriers equals the ratio of the average power of one intermodulation product with one of these difference frequencies to the average power of a signal with one of the fundamentals.

The third-order intermodulation distortions resulting from operation with more than three carriers are not worse than those resulting from operation with three carriers, but there are more intermodulation products. This may be determined either with a spectrum analyzer or mathematically. For n carriers the number of intermodulation products associated with the third-order intermodulation distortions $D_{3,2}$ and $D_{3,3}$ will be

$$n_{3,2} = n(n-1) \text{ and} \quad (4)$$

$$n_{3,3} = 0.5 n(n-1)(n-2) \quad (5)$$

Since the number of intermodulation products accordingly increases with n^2 and n^3 , a portion of the power in multi-carrier systems lies in the undesired sidebands. In Fig. 9 the power components of the carriers (and intermodulation products) calculated from the power ratio and the number of intermodulation products are plotted over the number of carriers.

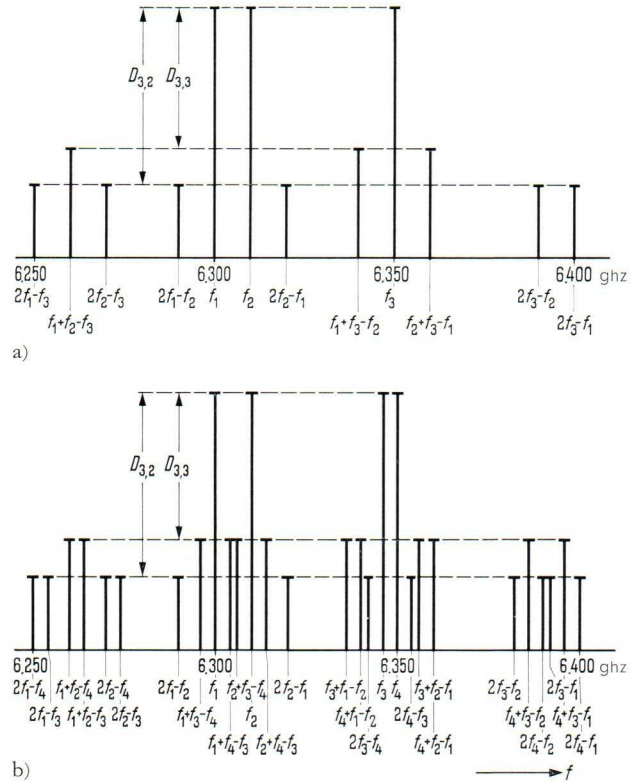


Fig. 8 Frequency spectra of a tube for (a) three-carrier operation and (b) four-carrier operation

Intermodulation distortion of traveling-wave tube YH 1041

Fig. 10 shows the total average output power of the tube YH 1041 as a function of the number of carriers n for various third-order intermodulation distortions $D_{3,2}$ or the 6-db less favorable values of $D_{3,3}$. If an intermodulation distortion of, say, 20 db is specified for a system operated with 6 carriers of equal power, the total power drawn from the tube YH 1041 must not exceed 1.5 kw (250 watts per carrier).

In measuring the third-order intermodulation distortion ($D_{3,2}$ and $D_{3,3}$) of a tube with a large output power, the test signals are usually preamplified with a single driver tube. The 20-watt traveling-wave tube RW 81 was used as a driver tube, for instance, for measurements on the tube YH 1041, and especially also in multi-carrier operation. The third-order intermodulation distortion measured behind the power tube is that of the cascaded driver and power tubes. In order to determine the true value of the modulation distortion $D_{3(P)}$ of the power tube, i.e. the value obtained when each input signal is preamplified with a separate driver tube, the value $D_{3(D+P)}$ measured at the output of the power tube must be corrected. This correction depends on the difference of two measurable third-order intermodulation distortions of the driver tube $D_{3(D)}$ and the cascade circuit $D_{3(D+P)}$. Fig. 11 shows the correction value (in db) required for determining the third-order intermodulation distortion of the power tube as a function of the measurable values of the third-order intermodulation distortion of the driver tube and the cascade circuit.

The blue curve in Fig. 4 shows the frequency response of the third-order intermodulation distortion $D_{3,2}$ for operation with two carriers spaced 5 Mhz apart and a total output power of 1.3 kw. Intercomparison with the

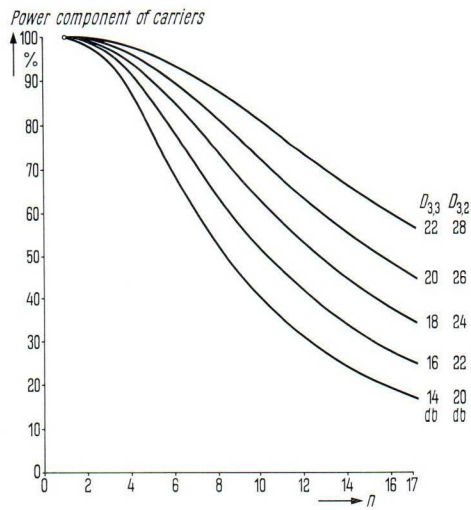


Fig. 9 Power components of carriers as a function of the number of carriers in multi-carrier operation (complement for 100% is always the power component of the intermodulation products) Parameter: third-order intermodulation distortion $D_{3,2}$, or the 6-db less favorable distortion $D_{3,3}$

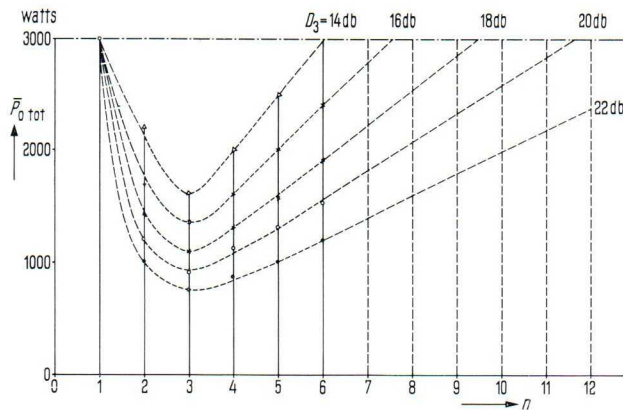


Fig. 10 Total average output power $\bar{P}_{0, \text{tot}}$ of tube YH 1041 as a function of the number of carriers. Parameter: third-order intermodulation distortion D_3 . Measuring points: $n = 1$ to 6 (f_1 to $f_6 = 6.34$ to 6.38 ghz)

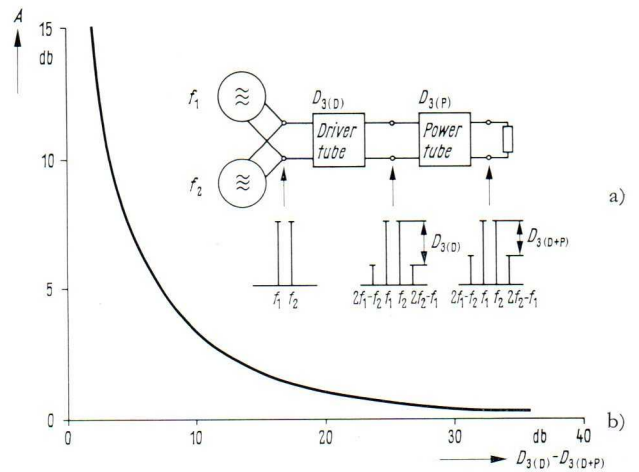
black curve (Fig. 4) shows that gain and intermodulation distortion have a similar frequency response. The reason for this is that the frequency response of both the gain and the intermodulation distortion is determined by the frequency-dependence of the coupling coefficient.

A further improvement of the intermodulation distortion may be realized by improving the coupling between the electron beam and the mode on the delay-line structure. Investigations of this nature are currently in progress.

With respect to the values given for the intermodulation distortion it should be added that it is still not known exactly what quality the intermodulation distortion must have with regard to the intermodulation noise on which the quality of transmission depends. Proper knowledge of this has yet to be obtained by experiment.

Variation of group delay in a 30-Mhz channel

As the result of a group delay $\Delta\tau$ in the frequency range $f_0 \pm \Delta f$ a frequency-modulated signal with the instantaneous frequency $f = f_0 + \Delta f \sin 2\pi f_m t$ (Δf frequency



a) Measuring circuit

$D_{3(D)}$ Third-order intermodulation distortion of driver tube
 $D_{3(P)}$ Third-order intermodulation distortion of power tube
 $D_{3(D+P)}$ Third-order intermodulation distortion of cascaded driver tube and power tube

b) Correction value A as a function of the values $D_{3(D)}$ and $D_{3(D+P)}$
 $D_{3(P)} = D_{3(D+P)} + A$

Fig. 11 Correction value A required for determining the value $D_{3(P)}$ from the measured values $D_{3(D+P)}$

deviation, f_m modulation frequency) experiences a frequency-dependent phase shift $\Delta\varphi$, i.e. its instantaneous frequency changes [6, 7].

In order to minimize distortion in the tube YH 1041 the dispersion of the first space harmonic of the mode with the longest wavelength is dimensioned for optimum frequency-independence. The group and phase delays in the frequency range of interest are therefore approximately equal. In addition, the internal reflections (multiple reflections) of the tube are minimized by carefully matching the attenuator and the coupling elements to the characteristic impedance of the delay line. Collectively, these measures ensure that the variation of the group delay of the tube YH 1041 will remain shorter than 2 nanosec within a 30 Mhz channel.

Harmonic power

Owing to the nonlinearities of a traveling-wave tube, harmonic power is also generated. In consequence, not only the signal power with a frequency f_i of the input signal and the powers of the intermodulation products but also harmonic power with the frequencies $(p+1)f_i$ may appear at the output of the tube ($p = 1, 2, \dots; p+1$ order of harmonic). The magnitude of the harmonic power depends both on the relative input loading of the tube and on the quality of synchronism between the electron beam and the waves of the frequencies $(p+1)f_i$, and the magnitude of the coupling impedance at these frequencies. The magnitude of the harmonic power also depends on the r-f matching of the delay line to the output-coupling waveguide. With the tube YH 1041 synchronism with waves of double the frequency of the input signal is possible, whereas the 3rd harmonic with the frequency $3f_i$ falls in a stopband of the circuit.

The largely frequency-dependent r-f coupling of the delay line in the harmonic region reduces the harmonic power at the output of the tube. According to the measurements recorded thus far, the power ratio between the fundamental and the 2nd harmonic

f	6	6.1	6.206	6.305	6.415	ghz
ΔG	$17 \cdot 10^{-3}$	$18 \cdot 10^{-3}$	$25 \cdot 10^{-3}$	$22 \cdot 10^{-3}$	$25 \cdot 10^{-2}$	db/Mhz
XTR	48.2	47.8	44.9	46	44.9	db

Table 3 Crosstalk ratios XTR of traveling-wave tube YH 1041

varies between 25 and 60 db when the tube is driven with a signal with a power of up to 3 kw. An improvement is realized with a harmonic filter developed by Siemens specifically for this application which suppresses harmonics down to about 50 db below the signal. Connected behind the tube, this filter damps the fundamental by only about 0.05 db.

Intelligible crosstalk

If two or more frequency-modulated signals are amplified simultaneously in a traveling-wave tube, frequency-dependent gain variations of the tube and a-m/p-m conversion produce intelligible crosstalk; the frequency-modulated signal undergoes amplitude modulation which is converted back into a frequency modulation through the a-m/p-m conversion characteristics of the tube. This is responsible for crosstalk between the baseband channels assigned to various carriers. The expected modulation can be estimated: a measure of this modulation is the crosstalk ratio XTR [8] which defines the ratio of the noise deviation of a disturbed (originally unmodulated) carrier to the frequency deviation of a disturbing (modulated) carrier. In the logarithmic scale, the crosstalk ratio is

$$XTR = 20 \log \left(\frac{\pi}{90} f_B \Delta G \epsilon_p \right) \quad (6)$$

where f_B denotes the baseband frequency in Mhz and ΔG the gain variation in db per Mhz: the coefficient ϵ_p (in deg/db) is referred to the average power.

Table 3 shows the crosstalk ratio values calculated for the tube YH 1041 on the basis of the respectively worst values for the frequency response of the gain, a baseband frequency of 5 Mhz and an a-m/p-m conversion coefficient of 1.3 deg/db (corresponding to a sum power of 1 kw).

Noise

For f-m radio relay systems, CCIR recommendations allow a certain noise power per voice channel. Part of this noise power derives from the transmitter tube. The noise of a traveling-wave tube is composed of amplitude noise and frequency noise.

The background noise power of the tube YH 1041 integrated over the frequency range of 5.925 to 13 ghz was

measured with a sensitive powermeter. It was found to be less than 0.2 mw.

The noise figure F when the tube is loaded with a signal is 37 to 40 db.

The frequency deviation $\sqrt{F^2}$ (mean square of variation) characterizing the frequency noise is determined with the equation [6, 9]

$$\sqrt{F^2} = f_m \sqrt{\frac{2kT_0FG(1+\epsilon_p^2)\Delta f}{P_0}} \quad (7)$$

where Δf denotes the channel width, f_m the modulation frequency, G the gain, P_0 the output power, k the Boltzmann constant and T_0 the absolute temperature. In the case of the a-m/p-m conversion coefficient, the angular change is expressed in radians and the power change of 1 db in a linear ratio. With the tube YH 1041 the frequency deviation is less than 3 hz and consequently almost without significance when $P_0 = 3$ kw, $f_m = 4$ Mhz, $\epsilon_p = 0.6$, $\Delta f = 4$ khz and the product $FG = 10^7$.

With 240 voice channels assigned to each CCIR channel, the noise contribution of the traveling-wave tube YH 1041 that is composed of these individual components is less than 50 picowatts.

Bibliography

- [1] Graf, H.: Die 2-kW-Senderendstufe der Erdefunkstelle Raisting. Siemens-Z. 40 (1966) pp. 7 to 11
- [2] Mayerhofer, E.; Meyerer, P.: YH 1040 Traveling-Wave Tube as Transmitting Amplifier at Raisting Earth Station. Siemens Rev. XXXII (1965) pp. 208 to 213
- [3] Mayerhofer, E.; Meyerer, P.: Neue Entwicklungen von Hochleistungs-Wanderfeldröhren. Siemens-Z. 40 (1966) pp. 317 to 319
- [4] Paschke, F.: New results on frequency multiplication and non-linear phase distortion in klystrons and traveling wave tubes. RCA Rev. 22 (1961) pp. 167 to 184
- [5] Laico, J.P.; McDowell, H.L.; Moster, C.R.: A medium-power traveling-wave tube for 6000-Mc radio relay systems. Bell Syst. techn. J. 35 (1956) pp. 1285 to 1346
- [6] Bretting, J.; Böhm, W.: Ein neuer permanentmagnetisch fokussierter Wanderfeldröhren-Verstärker für den Frequenzbereich von 4,4 bis 5 GHz. Telefunkenröhre No. 44 (1964) pp. 43 to 79
- [7] Brück, L.: Phasenverzerrungen bei der Verstärkung mit Laufeldröhren. Arch. elektr. Übertr. 7 (1953) pp. 28 to 36
- [8] Chapman, R.; Millard, J.B.: Intelligible crosstalk between frequency-modulated carriers through AM-PM conversion. Inst. Radio Engrs. Trans. Commun. Syst. 11 (1964) pp. 160 to 165
- [9] Liebscher, R.; Müller, R.: Frequency noise in traveling-wave tubes. Proc. Instn. Electr. Engrs. 105 (1958) Part B, suppl. 11, pp. 796 to 799